

Study of the Charmless Inclusive $B \rightarrow \eta' X$ Decay

G. Bonvicini,¹ D. Cinabro,¹ M. Dubrovin,¹ S. McGee,¹ A. Bornheim,² E. Lipeles,² S. P. Pappas,² A. Shapiro,² W. M. Sun,² A. J. Weinstein,² R. A. Briere,³ G. P. Chen,³ T. Ferguson,³ G. Tatishvili,³ H. Vogel,³ N. E. Adam,⁴ J. P. Alexander,⁴ K. Berkelman,⁴ V. Boisvert,⁴ D. G. Cassel,⁴ P. S. Drell,⁴ J. E. Duboscq,⁴ K. M. Ecklund,⁴ R. Ehrlich,⁴ R. S. Galik,⁴ L. Gibbons,⁴ B. Gittelman,⁴ S. W. Gray,⁴ D. L. Hartill,⁴ B. K. Heltsley,⁴ L. Hsu,⁴ C. D. Jones,⁴ J. Kandaswamy,⁴ D. L. Kreinick,⁴ A. Magerkurth,⁴ H. Mahlke-Krüger,⁴ T. O. Meyer,⁴ N. B. Mistry,⁴ J. R. Patterson,⁴ D. Peterson,⁴ J. Pivarski,⁴ S. J. Richichi,⁴ D. Riley,⁴ A. J. Sadoff,⁴ H. Schwarthoff,⁴ M. R. Shepherd,⁴ J. G. Thayer,⁴ D. Urner,⁴ T. Wilksen,⁴ A. Warburton,⁴ M. Weinberger,⁴ S. B. Athar,⁵ P. Avery,⁵ L. Brevva-Newell,⁵ V. Potlia,⁵ H. Stoeck,⁵ J. Yelton,⁵ K. Benslama,⁶ B. I. Eisenstein,⁶ G. D. Gollin,⁶ I. Karliner,⁶ N. Lowrey,⁶ C. Plager,⁶ C. Sedlack,⁶ M. Selen,⁶ J. J. Thaler,⁶ J. Williams,⁶ K. W. Edwards,⁷ D. Besson,⁸ X. Zhao,⁸ S. Anderson,⁹ V. V. Frolov,⁹ D. T. Gong,⁹ Y. Kubota,⁹ S. Z. Li,⁹ R. Poling,⁹ A. Smith,⁹ C. J. Stepaniak,⁹ J. Urheim,⁹ Z. Metreveli,¹⁰ K.K. Seth,¹⁰ A. Tomaradze,¹⁰ P. Zweber,¹⁰ S. Ahmed,¹¹ M. S. Alam,¹¹ J. Ernst,¹¹ L. Jian,¹¹ M. Saleem,¹¹ F. Wappler,¹¹ K. Arms,¹² E. Eckhart,¹² K. K. Gan,¹² C. Gwon,¹² K. Honscheid,¹² D. Hufnagel,¹² H. Kagan,¹² R. Kass,¹² T. K. Pedlar,¹² E. von Toerne,¹² M. M. Zoeller,¹² H. Severini,¹³ P. Skubic,¹³ S.A. Dytman,¹⁴ J.A. Mueller,¹⁴ S. Nam,¹⁴ V. Savinov,¹⁴ J. W. Hinson,¹⁵ J. Lee,¹⁵ D. H. Miller,¹⁵ V. Pavlunin,¹⁵ B. Sanghi,¹⁵ E. I. Shibata,¹⁵ I. P. J. Shipsey,¹⁵ D. Cronin-Hennessy,¹⁶ A.L. Lyon,¹⁶ C. S. Park,¹⁶ W. Park,¹⁶ J. B. Thayer,¹⁶ E. H. Thorndike,¹⁶ T. E. Coan,¹⁷ Y. S. Gao,¹⁷ F. Liu,¹⁷ Y. Maravin,¹⁷ R. Stroynowski,¹⁷ M. Artuso,¹⁸ C. Boulahouache,¹⁸ S. Blusk,¹⁸ K. Bukin,¹⁸ E. Dambasuren,¹⁸ R. Mountain,¹⁸ H. Muramatsu,¹⁸ R. Nandakumar,¹⁸ T. Skwarnicki,¹⁸ S. Stone,¹⁸ J.C. Wang,¹⁸ A. H. Mahmood,¹⁹ S. E. Csorna,²⁰ and I. Danko²⁰

(CLEO Collaboration)

¹Wayne State University, Detroit, Michigan 48202

²California Institute of Technology, Pasadena, California 91125

³Carnegie Mellon University, Pittsburgh, Pennsylvania 15213

⁴Cornell University, Ithaca, New York 14853

⁵University of Florida, Gainesville, Florida 32611

⁶University of Illinois, Urbana-Champaign, Illinois 61801

⁷Carleton University, Ottawa, Ontario, Canada K1S 5B6
and the Institute of Particle Physics, Canada M5S 1A7

⁸University of Kansas, Lawrence, Kansas 66045

⁹University of Minnesota, Minneapolis, Minnesota 55455

¹⁰Northwestern University, Evanston, Illinois 60208

¹¹State University of New York at Albany, Albany, New York 12222

¹²Ohio State University, Columbus, Ohio 43210

¹³University of Oklahoma, Norman, Oklahoma 73019

¹⁴University of Pittsburgh, Pittsburgh, Pennsylvania 15260

¹⁵Purdue University, West Lafayette, Indiana 47907

¹⁶University of Rochester, Rochester, New York 14627

¹⁷Southern Methodist University, Dallas, Texas 75275

¹⁸*Syracuse University, Syracuse, New York 13244*
¹⁹*University of Texas - Pan American, Edinburg, Texas 78539*
²⁰*Vanderbilt University, Nashville, Tennessee 37235*

(Dated: 05 March 2003)

Abstract

Based on a measurement of high momentum η' production in B decays, we determine the charmless inclusive $B \rightarrow \eta' X_{nc}$ branching fraction in the lab-frame momentum interval $2.0 < P_{\eta'} < 2.7$ GeV/ c . Using $9.7 \times 10^6 B\bar{B}$ pairs collected at the $\Upsilon(4S)$ center-of-mass energy with the CLEO II and II.V detector configurations, we find $\mathcal{B}(B \rightarrow \eta' X_{nc}) = [4.6 \pm 1.1 \pm 0.4 \pm 0.5] \times 10^{-4}$ in the $2.0 < P_{\eta'} < 2.7$ GeV/ c momentum range, where the uncertainties are statistical, systematic, and from subtraction of background from B decays to charm, respectively.

The flavor changing neutral current decays $b \rightarrow sg$ are forbidden at tree level in the Standard Model (SM), and hence at lowest order can only occur at the loop level. Interest in the charmless inclusive decay $B \rightarrow \eta' X$ (which we denote as $B \rightarrow \eta' X_{nc}$) arises because it is expected to be dominated by the $b \rightarrow sg$ transition followed by fragmentation of the gluon into η' via QCD anomaly coupling [1]-[7] and formation of multiparticle states X by the s quark. The amplitude of these gluonic penguin decays may receive significant contributions from diagrams with virtual non-SM particles in the loop.

CLEO previously reported an unexpectedly large rate for high momentum η' production from B decays [8]. That result was based on 4.7 fb^{-1} of total luminosity, taken both on the $\Upsilon(4S)$ resonance and at a center-of-mass energy 60 MeV below the resonance, which is below the $B\bar{B}$ production threshold. These datasets are referred to as “on-resonance” and “off-resonance” respectively. CLEO found an inclusive $B \rightarrow \eta' X_{nc}$ branching fraction [8] of $[6.2 \pm 1.6(\text{stat}) \pm 1.3(\text{syst})_{-1.5}^{+0.0}(\text{bkg})] \times 10^{-4}$ for $2.0 < P_{\eta'} < 2.7 \text{ GeV}/c$.

In this paper we present a new measurement of η' production from B decays in the momentum range $2.0 < P_{\eta'} < 2.7 \text{ GeV}/c$. Then, by subtracting background from B to charm decays, we use this result to determine $B \rightarrow \eta' X_{nc}$. The result is based on 9.1 fb^{-1} of on-resonance data and 4.4 fb^{-1} of off-resonance data. The analysis method is improved over CLEO’s previous $B \rightarrow \eta' X_{nc}$ analysis [8], and now uses a combination of the “pseudoreconstruction” and neural-network/shape-variable approaches that have been used in the CLEO analyses of $b \rightarrow s\gamma$ [9], [10]. These strategies are used to isolate the signal and to suppress the contribution from continuum η' production. We first search for $B \rightarrow \eta' X_{nc}$ candidates that are consistent with one of the B meson multiparticle decays. We then estimate the background from B decays to charm via Monte Carlo technique. These new results include the data used in the previous analysis and the results presented here supersede that measurement.

The data used for this analysis were collected with the CLEO detector [11] at the Cornell Electron Storage Ring, a symmetric e^+e^- collider. The CLEO detector measures charged particles over 95% of 4π steradians with a system of cylindrical drift chambers. (For 2/3 of the data used here, the innermost tracking chamber was a 3-layer silicon vertex detector.) Its CsI calorimeter covers 98% of 4π . Charged particles are identified by specific ionization measurement (dE/dx) in the outermost drift chamber and by time-of-flight counters placed just beyond the tracking volume. Muons are identified by their ability to penetrate the iron yoke of the magnet. Electrons are identified by the ratio of their shower energy to track momentum, by track-cluster matching, and by their shower shape.

We select events using a standard set of CLEO criteria for hadronic final states, and then search for candidate η' mesons by reconstructing the $\eta' \rightarrow \eta\pi^+\pi^-$, $\eta \rightarrow \gamma\gamma$ mode, where the $\gamma\gamma$ forming the η candidate must have an invariant mass within 30 MeV of the nominal η mass. We then form the mass difference between the reconstructed η' and η masses to improve resolution. The mass difference $M(\pi^+\pi^-\gamma\gamma) - M(\gamma\gamma)$ must be within 50 MeV of the nominal mass difference $\Delta M_{PDG} = M_{\eta'} - M_{\eta} = 410.5 \text{ MeV}$ [12]. We restrict the η' momentum to $P_{\eta'} > 1.6 \text{ GeV}/c$.

Using reconstruction we attempt to identify events in which a B decay produces a strange quark recoiling against an η' . The reconstruction is done by forming combinations of a charged kaon or a $K_S^0 \rightarrow \pi^+\pi^-$, an η' candidate, and n pions where $n \leq 4$ (at most one of these pions is allowed to be neutral); a total of eighteen decay modes and their charge conjugates are considered. For each B candidate we calculate the momentum P , energy E ,

and beam-constrained mass $M \equiv \sqrt{E_{beam}^2 - P^2}$. We then form the χ_B^2 of the reconstruction:

$$\chi_B^2 \equiv \left(\frac{E - E_{beam}}{\sigma_E} \right)^2 + \left(\frac{M - M_B}{\sigma_M} \right)^2,$$

where $\sigma_E = 40$ MeV and $\sigma_M = 4$ MeV.

We only consider candidates with $\chi_B^2 < 20$, and if an event has more than one candidate with $\chi_B^2 < 20$ we choose the candidate with the lowest χ_B^2 . This reconstructed X system may include strange, charm, or light quarks. Events with only light quarks in the recoil system ($X_{d(u)}$), however, will have slightly lower efficiency than the signal X_s cases. Events with charm in the recoil system will have comparable efficiency to the X_s cases, and we will later subtract these as background. In cases where all decay products of X are identified correctly (50% of the time) the X mass ($M(X)$) resolution varies from 20 to 30 MeV for low and high $M(X)$ respectively. The $M(X)$ resolution becomes 200 to 300 MeV if there are missing or extra particles in the X reconstruction. Given a reconstructed candidate, we use χ_B^2 and $|\cos \theta_{tt}|$ as variables for continuum suppression, where θ_{tt} is the angle between the thrust axis of the candidate B and the thrust axis of the rest of the event.

We also use event shape variables and the presence or absence of a lepton (electron or muon) to further suppress the continuum background. Specifically, we use a neural network optimized on signal and continuum Monte Carlo to combine the following event shape variables into a single variable r_{shape} : the normalized Fox-Wolfram second moment R_2 [13], S_{\perp}^1 , and the energies in 20° and 30° cones, parallel and antiparallel to the η' direction. If the event contains a lepton then we also use the momentum of the lepton, P_l , and the angle between the lepton and the η' , $\theta_{l\eta'}$.

We thus have two types of events: those with both a pseudoreconstruction and a lepton, for which we use r_{shape} , χ_B^2 , $|\cos \theta_{tt}|$, P_l , and $\theta_{l\eta'}$; and events with only a pseudoreconstruction, for which we use r_{shape} , χ_B^2 , and $|\cos \theta_{tt}|$. For each of these two cases the available variables are combined using a neural network that has been optimized using signal and continuum Monte Carlo samples. For each of the two resulting networks, we can maximize the statistical strength by converting the network output r into a weight, $w(r) = s(r)/[s(r) + (1+a)b(r)]$, where $s(r)$ and $b(r)$ are the expected yields for signal and for continuum background respectively, r is the net output, and a is the luminosity scale factor between on-resonance and off-resonance data samples ($a \approx 2.0$).

The above choice of weights minimizes the expected statistical error on the $B \rightarrow \eta' X_{nc}$ yield after off-resonance subtraction. To reduce the systematic error that arises from having some efficiency dependence on the reconstructed $M(X)$ value, however, we adjust the weight event-by-event based on the measured value of $M(X)$. The factor for this adjustment was obtained from signal Monte Carlo by fitting the measured efficiency dependence on $M(X)$ to a straight line. By using these adjusted weights we slightly increase our expected statistical error, but decrease a systematic error.

We obtain yields from both on- and off-resonance data by fitting the distributions of the mass difference $M(\pi^+\pi^-\gamma\gamma) - M(\gamma\gamma) - \Delta M_{PDG}$. We use Gaussian and linear functions for the η' signal and combinatorial background respectively. In these fits, we constrain the mean of the Gaussian to be zero, and the width to be 4.0 MeV based on Monte Carlo simulation.

¹ S_{\perp} is defined as the sum of the magnitudes of components of momenta perpendicular to the direction of the η' for all particles more than 45° from the η' axis, divided by the sum of the magnitudes of momenta of all particles other than the η' .

We scale the off-resonance yield by the on to off ratio of \mathcal{L}/E_{cm}^2 to account for luminosity and cross-section differences between the two datasets. We also scale particle momenta by the on/off energy ratio to account for the small energy difference between the on-resonance and off-resonance data². We then find our $B \rightarrow \eta' X$ yield by subtracting this off-resonance yield from the on-resonance yield. The mass difference $M(\pi^+\pi^-\gamma\gamma) - M(\gamma\gamma) - \Delta M_{PDG}$ in the η' momentum range $2.0 < P_{\eta'} < 2.7$ GeV/ c is shown in Figure 1, and yields from fits are tabulated in Table I. We estimate a systematic error of 3% from the uncertainty in the fitting procedure.

To search for $B \rightarrow \eta' X_{nc}$, we take as signal the momentum region $2.0 < P_{\eta'} < 2.7$ GeV/ c because it is above the kinematic limit for most B to charm decays. Some B to charm decays, however, will still enter this signal region. We estimate this background by using $B\bar{B}$ Monte Carlo events and by measuring the data yield in a control region of $1.6 < P_{\eta'} < 1.9$ GeV/ c , chosen because here we expect $B \rightarrow \eta' X_{nc}$ to be much smaller than B decays to charm. The estimated yields from B backgrounds are tabulated in Table I. The continuum-subtracted and combinatorial-background-subtracted $M(X)$ distribution is shown in Figure 2. Cascade decays (e.g., $B^0 \rightarrow D_{(s)}X, D_{(s)} \rightarrow \eta' Y$) and color allowed decays ($b \rightarrow cW, W \rightarrow \eta' + (n\pi)$) have been simulated in the CLEO $B\bar{B}$ Monte Carlo. We do not use this Monte Carlo prediction directly; instead, we rescale the CLEO $B\bar{B}$ Monte Carlo yield in the signal region by the factor of 1.06 ± 0.22 to account for half of the difference between data and Monte Carlo in the control region. We include the statistical and systematic uncertainties from the control region in the error on the scale factor. We estimate the yield of color suppressed decays with a Monte Carlo sample that assumed the following branching fractions: $\mathcal{B}(B^0 \rightarrow \eta' D^0 + \eta' D^{0*}) = (3.1 \pm 0.9) \times 10^{-4}$ [14] and $\mathcal{B}(B^0 \rightarrow \eta' D^{0**}) = 1/2 \mathcal{B}(B^0 \rightarrow \eta' D^0 + \eta' D^{0*}) = 1.55 \times 10^{-4}$. We take the error on $\mathcal{B}(B^0 \rightarrow \eta' D^{0**})$ to be 50% of itself. We use the modified ISGW model [15] for the mass distribution of D^{0**} .

We determine the efficiency — defined as weights per $B \rightarrow \eta' X_{nc}$ event generated in the momentum range $2.0 < P_{\eta'} < 2.7$ GeV/ c — via Monte Carlo simulation. The hadronization of the quark pair into X_s or $X_{d(u)}$ is done by the JETSET Monte Carlo. We use a uniform X_{nc} mass distribution for the multiparticle final states, and assume that the branching fraction for $B \rightarrow \eta' K$ is one eighth of the total branching fraction $B \rightarrow \eta' X_s$ in this momentum range [16],[8]. The detection efficiency is averaged over charged and neutral B mesons and corrects for unobserved modes with neutral kaons ($K_L^0, K_S^0 \rightarrow \pi^0\pi^0$), for modes with a charged kaon and more than one π^0 in the final state, and for final states with baryons; it also includes the product of branching fractions $\mathcal{B}(\eta' \rightarrow \eta\pi^+\pi^-) \times \mathcal{B}(\eta \rightarrow \gamma\gamma) = 16.96\%$.

To estimate the uncertainty in efficiency due to the choice of a uniform shape for the $M(X_{nc})$ distribution, we vary the shape of the $M(X_{nc})$ distribution for the multiparticle final states from uniform to linear with intercept at the $K - \pi$ threshold, keeping the fraction of $B \rightarrow \eta' K$ constant; this leads to a systematic error of 6.3%. The systematic error on the efficiency includes 3.3% uncertainty from the event modeling of $B \rightarrow \eta' X_{nc}$ which includes uncertainties in event shape, hadronization, and other- B modeling, and 2.1% uncertainty from the detector performance which includes uncertainties in the detection efficiencies and resolutions for tracks and photons.

To obtain the $B \rightarrow \eta' X_{nc}$ branching fraction, we take the background-subtracted yield in the momentum range $2.0 < P_{\eta'} < 2.7$ GeV/ c of $61.2 \pm 13.9 \pm 6.6$ weights, where the first

² The on- and off-resonance datasets have center-of-mass energies of 10.58 and 10.52 GeV respectively.

error is statistical and the second is from uncertainty in the subtraction of the B to charm decay background. The efficiency is $(6.81 \pm 0.56) \times 10^{-3}$ weights per event, where the error results from dependence of efficiency on the $M(X_{nc})$ distribution, from X_{nc} hadronization, from other- B modeling, and from detector performance. Our sample contains 9.7 million $B\bar{B}$ pairs ($\pm 2\%$). We obtain $\mathcal{B}(B \rightarrow \eta' X_{nc}) = [4.6 \pm 1.1(\text{stat}) \pm 0.4(\text{syst}) \pm 0.5(\text{bkg})] \times 10^{-4}$ for $2.0 < P_{\eta'} < 2.7$ GeV/ c .

Also included in our measured branching fraction are components from $b \rightarrow dg$ gluonic penguin decays and $b \rightarrow u$ tree level decays. Within the SM, the contribution from these decays is expected to be of the order of a few per cent of the $B \rightarrow \eta' X_{nc}$ rate. We determine that the ratio of efficiencies for the final states that consist only of d and u quarks to the final states that contain s quark is 0.79. Thus, the branching fraction we have measured is a weighted sum of branching fractions $\mathcal{B}(B \rightarrow \eta' X_{nc}) = \mathcal{B}(B \rightarrow \eta' X_s) + 0.79 \mathcal{B}(B \rightarrow \eta' X_{d(u)})$.

In summary, we have updated the measurement of the charmless inclusive decay $B \rightarrow \eta' X_{nc}$ for $2.0 < P_{\eta'} < 2.7$ GeV/ c using the CLEO II and II.V data sets which contain 9.7 million $B\bar{B}$ pairs. This result is in agreement with CLEO's previous inclusive measurement and hence confirms its unexpectedly large rate. CLEO has also previously measured [16] the exclusive decay $B \rightarrow \eta' K$ using the same dataset as the results we report here; that result is therefore not statistically independent of our new results.

The large $B \rightarrow \eta' X_{nc}$ rate can be understood if the $b \rightarrow sg$ rate is larger than expected in the Standard Model [2]. A number of alternative explanations, however, have also been proposed. One of these is the QCD anomaly mechanism $b \rightarrow sg, g \rightarrow \eta' g$ with the $\eta' gg$ form-factor being a slowly-falling function of the gluon Q^2 [1]. A slowly-falling $\eta' gg$ form-factor, however, is strongly disfavored by the recent CLEO measurement of the $\Upsilon(1S) \rightarrow \eta' X$ spectrum [17]; a rapidly-falling form-factor needed for consistency with the $\Upsilon(1S) \rightarrow \eta' X$ result predicts a $B \rightarrow \eta' X$ rate of 3×10^{-5} [18], which is an order of magnitude smaller than observed. Another possible explanation of the high rate for $B \rightarrow \eta' X_{nc}$ is that the η' has a substantial intrinsic charm content [6]. In this case the η' can be produced by the axial vector part of the $b \rightarrow (c\bar{c})s$ process. This explanation is also disfavored by CLEO measurements. First, the $B \rightarrow \eta_c K$ rate is not enhanced relative to the $B \rightarrow J/\psi K$ rate [19]. Further, this explanation requires that the $B \rightarrow \eta' K^*$ rate be roughly half the $B \rightarrow \eta' K$ rate [4],[6], which is inconsistent with observations [16],[20].

We gratefully acknowledge the effort of the CESR staff in providing us with excellent luminosity and running conditions. M. Selen thanks the Research Corporation, and A.H. Mahmood thanks the Texas Advanced Research Program. This work was supported by the National Science Foundation, and the U.S. Department of Energy.

η' Momentum Range (GeV/ c)	1.6 - 1.9	2.0 - 2.7
ON	251.8 ± 25.9	149.4 ± 11.4
$a \times \text{OFF}$	90.8 ± 15.3	55.3 ± 7.9
ON $-a \times \text{OFF}$	161.0 ± 30.0	94.1 ± 13.9
Color suppressed decays		
$B^0 \rightarrow \eta' D^0 + \eta' D^{0*}$	0.0 ± 0.1	17.4 ± 5.0
$B^0 \rightarrow \eta' D^{0**}$	2.8 ± 0.2	1.4 ± 0.7
CLEO $B\bar{B}$ Monte Carlo	140.6 ± 11.0	13.3 ± 2.9
Scaled by control region		14.1 ± 4.3
Sum of B backgrounds	143.4 ± 11.0	32.9 ± 6.6
ON $-a \times \text{OFF}-B$ backgrounds	$17.6 \pm 30.0(\text{stat})$	$61.2 \pm 13.9(\text{stat})$

TABLE I: Yields(weights) from the fit in the signal ($2.0 < P_{\eta'} < 2.7$ GeV/ c) and control ($1.6 < P_{\eta'} < 1.9$ GeV/ c) regions. Given are yields on-resonance, scaled off-resonance, on minus scaled off, estimated background from color suppressed B decays, estimated background from cascade and color allowed B decays, sum of B backgrounds, and on minus scaled off minus B backgrounds. The error on the continuum-subtracted and B -backgrounds-subtracted yield is statistical only and does not include the error from the background subtraction.

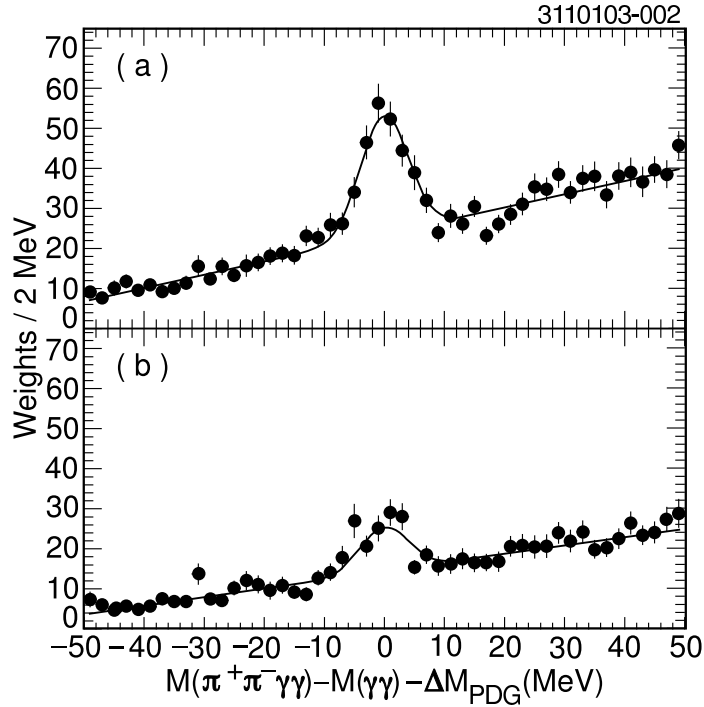


FIG. 1: The distribution of $M(\pi^+\pi^-\gamma) - M(\gamma) - \Delta M_{PDG}$ in the signal region $2.0 < P_{\eta'} < 2.7$ GeV/ c for (a) on-resonance data and (b) scaled off-resonance data.

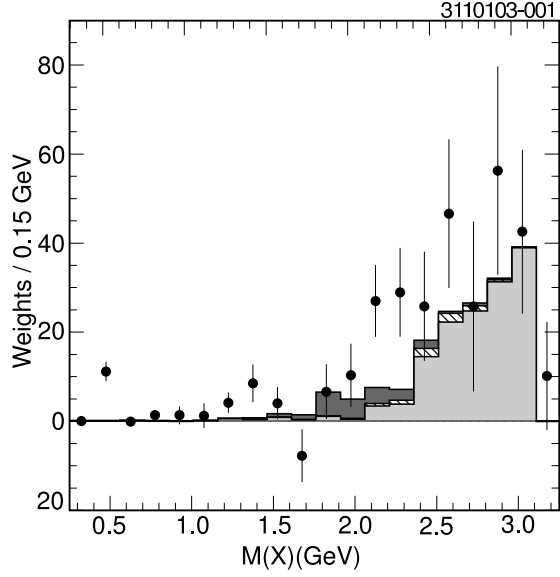


FIG. 2: The continuum-subtracted and combinatorial-background-subtracted $M(X)$ distribution (points with error bars) with estimated background from B decays to charm (histogram). The various contributions are cascade decays (light grey) and color suppressed decays $B^0 \rightarrow \eta' D^0 + \eta' D^{0*}$ (dark grey) and $B^0 \rightarrow \eta' D^{0**}$ (hatched area). Ignoring the small smearing effects from the boosted B mesons ($300 \text{ MeV}/c$), the mass ranges $M(X) < 2.35 \text{ GeV}$ and $M(X) > 2.5 \text{ GeV}$ correspond to momentum ranges in Table I of $P_{\eta'} > 2.0 \text{ GeV}/c$ and $P_{\eta'} < 1.9 \text{ GeV}/c$ respectively.

-
- [1] D. Atwood and A. Soni, Phys. Rev. Lett. **79**, 5206 (1997).
- [2] A. L. Kagan and A. A. Petrov, arXiv:hep-ph/9707354.
- [3] H. Fritzsch, Phys. Lett. B **415**, 83 (1997).
- [4] W. S. Hou and B. Tseng, Phys. Rev. Lett. **80**, 434 (1998).
- [5] X. G. He and G. L. Lin, Phys. Lett. B **454**, 123 (1999).
- [6] I. E. Halperin and A. Zhitnitsky, Phys. Rev. Lett. **80**, 438 (1998); Phys. Rev. D **56**, 7247 (1997).
- [7] A. Ali and A. Y. Parkhomenko, DESY 01-012 [arXiv:hep-ph/0112048].
- [8] T. E. Browder *et al.* [CLEO Collaboration], Phys. Rev. Lett. **81**, 1786 (1998).
- [9] J. A. Ernst, Ph.D. thesis, University of Rochester (1995).
- [10] S. Chen *et al.* [CLEO Collaboration], Phys. Rev. Lett. **87**, 251807 (2001).
- [11] Y. Kubota *et al.* [CLEO Collaboration], Nucl. Instrum. Methods Phys. Res., Sect. A **320**, 66 (1992); T. Hill, Nucl. Instrum. Methods Phys. Res., Sect. A **418**, 32 (1998).
- [12] K. Hagiwara *et al.* [Particle Data Group Collaboration], Phys. Rev. D **66**, 010001 (2002).
- [13] G. Fox and S. Wolfram, Phys. Rev. Lett. **41**, 1581 (1978).
- [14] Preliminary result of an independent CLEO study of the color suppressed $B \rightarrow \eta' D^{0(*)}$ decays.
- [15] N. Isgur, D. Scora, B. Grinstein and M. B. Wise, Phys. Rev. D **39**, 799 (1989).
- [16] S. J. Richichi *et al.* [CLEO Collaboration], Phys. Rev. Lett. **85**, 520 (2000).
- [17] M. Artuso *et al.* [CLEO Collaboration], Phys. Rev. D (to be published) [arXiv:hep-ex/0211029].
- [18] A. L. Kagan, AIP Conf. Proc. **618**, 310 (2002) [arXiv:hep-ph/0201313].
- [19] K. W. Edwards *et al.* [CLEO Collaboration], Phys. Rev. Lett. **86**, 30 (2001).
- [20] B. Aubert *et al.* [BABAR Collaboration], SLAC-PUB-8914 [arXiv:hep-ex/0107037].